

AIR FORCE
TECHNICAL DATA CENTER

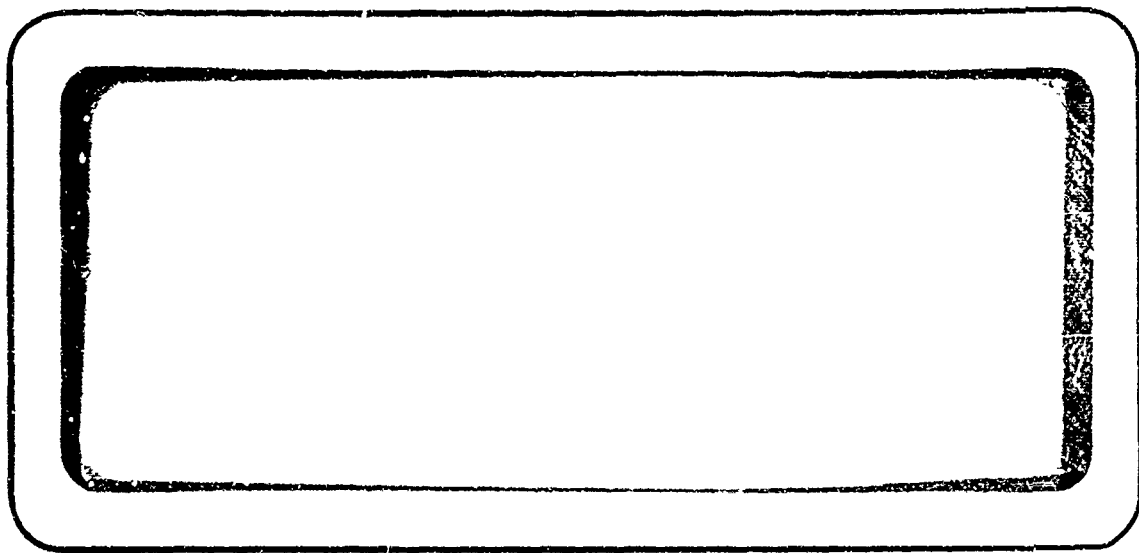
TECHNICAL LIBRARY

120

Document No. _____

Copy No. _____

AD 607696



COPY	1	OF	1	leaf
HARD COPY				\$ 3.00
MICROFICHE				\$ 0.50

54p



SPACE TECHNOLOGY LABORATORIES, INC.

ARCHIVE COPY

DDC
RECEIVED
NOV 4 - 1964

AD 607696

RE-ENTRY VEHICLE SYNTHESIS PROGRAM

T. L. Petersen


✓ STL/TR-60-0000-09103

April 21, 1960

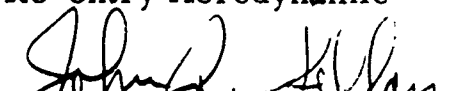
Prepared


T. L. Petersen

Approved


A. Ambrosio, Head
Re-entry Aerodynamic

Approved


J. R. Sellars, Manager
Aerodynamics Department

SPACE TECHNOLOGY LABORATORIES, INC.
P.O. Box 95001
Los Angeles 45, California

611 7570

ABSTRACT

This report describes the current re-entry vehicle parametric study program, based on the Allen and Eggers straight line trajectory assumptions. The heating analysis considers a nonreacting cold wall, with the inclusion of a moving boundary conduction solution and boundary layer transition. The quantities determined are ablation thicknesses, insulation thicknesses, vehicle weight and aerodynamic coefficients, for varying shape, material and trajectory parameters. The computer output consists only of final integrated values rather than step-by-step computations along the trajectory.

ACKNOWLEDGEMENTS

The Re-entry Vehicle Synthesis Program is the work in varying degrees of all the members of the Re-entry Aerodynamics Section. Those especially responsible are A. Ambrosio, D.H. Baer, and T.R. Thompson.

CONTENTS

	Page
I. INTRODUCTION.	1
II. TRAJECTORY EQUATIONS	2
III. THERMODYNAMIC ASSUMPTIONS	2
IV. LAMINAR CONVECTIVE HEATING	3
V. TURBULENT CONVECTIVE HEATING	5
VI. TRANSITION FROM LAMINAR TO TURBULENT FLOW . . .	7
VII. HEAT SHIELD AND INSULATION THICKNESSES	9
VIII. VEHICLE GEOMETRY	11
IX. FIXED WEIGHT AND PAYLOAD	13
X. MACHINE COMPUTATIONS	14
XI. FLOW DIAGRAMS	25

DEFINITION OF SYMBOLS

Symbol

A	Frontal area
C_D	Drag coefficient
$C_D^{(N)}$	Newtonian drag coefficient
C_1, C_2, \dots	Computational constants
C_M	Coefficient of moment about pitch axis
C_N	Coefficient of moment about yaw axis
C_P	Specific heat
d_{SR}	Stiffener ring depth
E	Modulus of elasticity
f_{SR}	Safety factor
g	32.284 ft/sec ²
H	Total enthalpy
h	Specific enthalpy
I_R, I_P	Roll, pitch moment of inertia
I_x	Pitch moment of inertia with respect to plane normal to the x axis through the origin.
K	Experimental constant
K_1, K_2, K_3	Computational constants
k	Coefficient of thermal conductivity
L	Latent heat of sublimation
N_{TR}	Transition parameter
n	Number of computational intervals in a given section
P	Pressure
Q, Q_T	Total heat transferred to the body at any point

Q^*	Average cold wall heat absorption capability
\dot{q}	Heat flux
\dot{q}_m	Heat flux at time t_o
R	Radius
R_E	Reynolds number based on laminar boundary layer momentum thickness
r	Radial coordinate
T	Temperature
T_i	Maximum permissible temperature on inside of wall at end of ablation
T_o	Initial temperature
T_s	Ablation temperature
t	Time
t_f	Total heating time
u	Velocity
V_o	Normalized velocity constant
V^*	Dimensionless ablation rate
W	Weight
x	Longitudinal body position coordinate
\bar{x}	x coordinate of center of gravity
$x_{C.P.}$	x coordinate of center of pressure
x_T	Total wall thickness
Y	Altitude
y	Coordinate normal to body
α	Thermal diffusivity
β	Scale height in atmospheric density-altitude relationship = $4.5 \times 10^{-5}/ft$
γ	Ratio of specific heats
Δ	Ballistic coefficient = $W/C_D A$

δ	Boundary layer thickness
θ, θ_B	Body angles
θ_E	Re-entry angle of trajectory with horizontal
μ	Coefficient of viscosity
ρ	Density
$\bar{\rho}$	Reference density in atmospheric density-altitude relationship
σ_{SR}	Thickness/depth ratio of stiffener ring
τ	Material thickness
ϕ	Body angle

Subscripts

B	Base
E	Re-entry
L	Laminar
M	Material
N	Nose
o	Stagnation
P	Cover plate
P/L	Payload
q	Partial derivative with respect to roll velocity
t	Turbulent
w	Wall
α	Partial derivative with respect to angle of attack
δ	Edge of boundary layer
∞	Free stream
CO	Cutoff
C.W.	Cold wall
H.S.	Heat sink
H.S. ABL.	Heat sink ablated
H.S. MAX.	Total heat sink
H.S. RES.	Heat sink residual
INS.	Insulation
P/L	Payload
SR	Stiffener ring
ST	Structure
TOT	Total
TR	Transition
R	Reference

I. INTRODUCTION

The purpose of this report is to serve as an aid in running the IBM 704 Re-entry Vehicle Synthesis Program for parametric design studies of re-entry vehicles. The report is essentially divided into two parts: the first part presents the basic equations that are utilized and the assumptions that have been made, while the second (sections IX and X) deals with the actual computational procedure that the machine uses to solve the equations for the first part in the case of a given re-entry vehicle. A straight line trajectory is assumed and the heating analysis is for the case of a non-reacting cold wall, with heat conduction into the wall and boundary layer transition. The computer output consists of values of ablation and insulation thicknesses, vehicle weight, and aerodynamic coefficients. All of the heat equations were integrated over the trajectory prior to programming so that the computer output consists only of total rather than step-wise values.

II. TRAJECTORY EQUATIONS⁽¹⁾

The following trajectory equations were derived by Allen and Eggers⁽²⁾ under the assumptions of constant drag coefficient, negligible gravitational effects, and an exponential variation of atmospheric density with altitude:

$$u_{\infty} = u_E \exp \left[\frac{-\bar{\rho} g e^{-\beta Y}}{2\beta \left(\frac{W}{C_D A} \right) \sin \theta_E} \right] \quad (1)$$

where

$$\rho = \bar{\rho} e^{-\beta Y}$$

$$\frac{du_{\infty}}{dt} = -\beta \sin \theta_E u_{\infty}^2 \ln \frac{u_E}{u_{\infty}} \quad (2)$$

$$\rho_{\infty} = \frac{2\beta}{g} \left(\frac{W}{C_D A} \right) \sin \theta_E \ln \frac{u_E}{u_{\infty}} \quad (3)$$

III. THERMODYNAMIC ASSUMPTIONS⁽¹⁾

- a) The air passing over the vehicle is a dissociated gas in thermal equilibrium.
- b) The conditions at the edge of the boundary layer at any point along the body can be computed from the stagnation point conditions by means of an isentropic expansion, since the energy losses to the body are relatively small.
- c) The viscosity varies as the square root of the enthalpy.
- d) An average value of $\gamma = 1.2$ will be used.

Under these assumptions the following relationships hold:

$$\left(\frac{p_\delta}{p_o}\right) = \left(\frac{P_\delta}{P_o}\right)^{1/\gamma} \quad (4)$$

$$\frac{u_\delta}{\sqrt{2h_o}} = \left\{ 1 - \left(\frac{P_\delta}{P_o}\right)^{\frac{\gamma-1}{\gamma}} \right\}^{1/2} \quad (5)$$

$$\frac{\mu_\delta}{\mu_o} = \left(\frac{h_\delta}{h_o}\right)^{1/2} = \left(\frac{P_\delta}{P_o}\right)^{\frac{\gamma-1}{2\gamma}} \quad (6)$$

IV. LAMINAR CONVECTIVE HEATING⁽¹⁾

The basic equation to be solved is

$$\dot{q}_L = k_w \left(\frac{\partial T}{\partial y} \right)_w \quad (7)$$

This equation can be transformed by using the Levy transformation combined with the Mangler transformation for bodies of revolution. The following assumptions are made:

a) The variation of heat transfer rate with local pressure gradients is negligible.

b) $\rho\mu$ may be assumed constant across the boundary layer if evaluated at some average enthalpy.

c) The free stream static enthalpy is negligible.

Under these assumptions the laminar cold wall convective heating rate can be written as

$$\dot{q}_L = C_1 u_\infty^2 \left(\rho_o \mu_o \sqrt{h_o} \right)^{1/2} \left(\frac{1}{R_B} \right)^{1/2} F_1 \left(\frac{r}{R_B} \right) \quad (8)$$

where $F_1(r/R_B)$ represents the variation of local heating rate around the vehicle and is a function of geometry and pressure:

$$F_1\left(\frac{r}{R_B}\right) = \frac{\left(\frac{r}{R_B}\right) \left(\frac{P_\delta}{P_o}\right)^{\frac{\gamma+1}{2\gamma}} \left\{1 - \left(\frac{P_\delta}{P_o}\right)^{\frac{\gamma-1}{\gamma}}\right\}^{1/2}}{\left\{\int_0^{r/R_B} \left(\frac{r}{R_B}\right)^2 \left(\frac{P_\delta}{P_o}\right)^{\frac{\gamma+1}{2\gamma}} \left\{1 - \left(\frac{P_\delta}{P_o}\right)^{\frac{\gamma-1}{\gamma}}\right\}^{1/2} \frac{d(r/R_B)}{\sin \theta_B}\right\}^{1/2}} \quad (9)$$

The limit of this expression at the stagnation point $r = 0$ is found to be:

$$F_1(0) = 2 \left(\frac{R_B}{R_N}\right)^{1/2} \left(\frac{\gamma-1}{\gamma}\right)^{1/4} \quad (10)$$

By equation (6) μ_o can be expressed as a function of u_∞ . An approximate expression for ρ_o/ρ_∞ was determined as a function of , from gas tables:

$$\frac{\rho_o}{\rho_\infty} = C_2 u_\infty^n \quad (11)$$

From the above relationships and equation (2), the time-dependent variables in equation (8) can be expressed in terms of u_∞ . Integration of the resulting equation from the initial value of $u_\infty = u_E$ to any arbitrary value of u_∞ gives the total laminar convective heat transfer per unit area as

$$Q_L = K_L \left(\frac{W}{C_{DA} R_N}\right)^{1/2} \left(\frac{\gamma}{\gamma-1}\right)^{1/4} \left(\frac{R_N}{R_B}\right)^{1/4} F_1\left(\frac{r}{R_B}\right) \operatorname{erf} \sqrt{2.152 \ln \frac{u_E}{u_\infty}} \quad (12)$$

where

$$K_L = K'_L u_E^{2.152} (\sin \theta_E)^{-1/2}$$

and K'_L is an experimentally determined constant.

V. TURBULENT CONVECTIVE HEATING⁽¹⁾

In this case the basic equation to be solved is the integral form of the energy equation:

$$\frac{d}{dx} \left\{ \delta \int_0^1 r \rho u (H - H_\delta) d \left(\frac{y}{\delta} \right) \right\} = - r \dot{q}_w \quad (13)$$

The wall heating rate may be computed from the Blasius turbulent flat plate solutions in the form:

$$\dot{q}_t = C_3 \rho u (Re_\delta)^{-1/4} (H_\delta - H_w) \quad (14)$$

where Re_δ is defined as

$$Re_\delta = \frac{\rho u \delta}{\mu} \quad (15)$$

It is assumed that ρu and H vary with y/δ as follows:

$$\frac{\rho u}{\rho_\delta u_\delta} = \frac{H - H_w}{H_\delta - H_w} = \left(\frac{y}{\delta} \right)^{1/7} \quad (16)$$

This yields an expression for δ which can then be substituted into equation (13) to give the turbulent convective heating rate. If the starting length is measured from the nose, the turbulent heating rate can be written as:

$$\dot{q}_t = \frac{C_3 \rho' u (\mu')^{1/4} (H_\delta - H_w)}{\left[C_4 \int_0^x r^{5/4} \rho' u (\mu')^{1/4} dx \right]^{1/5}} \quad (17)$$

If ρ' , μ' are the values of ρ , μ evaluated at some average enthalpy

to include compressibility effects across the boundary layer, and the ratio $\rho' (\mu')^{1/4} / \rho \mu^{1/4}$ is averaged along the body, the equation (17) becomes:

$$\dot{q}_t = C_5 \left[\frac{(\rho_o \sqrt{h_o})^4 \mu_o}{R_B} \right]^{1/5} \frac{u_\infty^2}{2} F_2 \left(\frac{r}{R_B} \right) \quad (18)$$

where

$$F_2 \left(\frac{r}{R_B} \right) = \frac{\left(\frac{r}{R_B} \right)^{1/4} \left(\frac{P_\delta}{P_o} \right)^{\frac{\gamma+7}{8\gamma}} \left[1 - \left(\frac{P_\delta}{P_o} \right)^{\frac{\gamma-1}{\gamma}} \right]^{1/2}}{\left\{ \int_0^{r/R_B} \left(\frac{r}{R_B} \right)^{5/4} \left(\frac{P_\delta}{P_o} \right)^{\frac{\gamma+7}{8\gamma}} \left[1 - \left(\frac{P_\delta}{P_o} \right)^{\frac{\gamma-1}{\gamma}} \right]^{1/2} \frac{d(r/R_B)}{\sin \theta_B} \right\}^{1/5}} \quad (19)$$

As in the case of laminar heating, the quantities ρ_o , h_o , μ_o can be expressed in terms of u_∞ , and the resulting equation for q_t integrated to yield an expression for the total turbulent heating per unit area:

$$Q_t = K_t \left(\frac{W}{C_{DA}} \right)^{4/5} \left(\frac{1}{R_B} \right)^{1/5} F_2 \left(\frac{r}{R_B} \right) \left[\Gamma_X^{(4/5)} - \Gamma_{X_{TR}}^{(4/5)} \right] \quad (20)$$

where

$$K_t = K'_t u_E^{2.485} (\sin \theta_E)^{-1/5}$$

and K'_t is an experimentally determined constant $\Gamma_X^{(4/5)}$ represents the incomplete gamma function with $X = 2.4853 \ln u_E / u_{\infty_{TR}}$. It should be noted that there is a stronger dependence on (W/C_{DA}) in turbulent flow than in laminar flow.

VI. TRANSITION FROM LAMINAR TO TURBULENT FLOW

The transition criterion selected for this program is based on the momentum thickness Reynold's number which is given by

$$R_{e\theta} = \frac{0.66}{r\mu_\delta} \sqrt{\int_0^x \rho_\delta u_\delta \mu_\delta r^2 dx} \quad (21)$$

Substituting (4), (5), and (6) into (21) gives

$$R_{e\theta} = 0.785 \sqrt{\frac{\rho_o \sqrt{h_o}}{\mu_o}} F_3 \left(\frac{r}{R_B} \right) \quad (22)$$

where

$$F_3 \left(\frac{r}{R_B} \right) = \frac{\sqrt{R_B \int_0^{r/R_B} \left(\frac{r}{R_B} \right)^2 \left(\frac{P_\delta}{P} \right)^{\frac{\gamma+1}{2\gamma}} \sqrt{1 - \left(\frac{P_\delta}{P_o} \right)^{\frac{\gamma-1}{\gamma}} \frac{d(r/R_B)}{\sin \theta_B}}}}{\left(\frac{r}{R_B} \right) \left(\frac{P_\delta}{P_o} \right)^{\frac{\gamma-1}{2\gamma}}} \quad (23)$$

(22) may be re-written as

$$\left(\frac{R_{e\theta}}{F_3} \right)^2 = (0.785)^2 \frac{\frac{\rho_o}{\rho_\infty} \sqrt{h_o}}{\frac{\mu_o}{\mu_R}} \frac{\rho_\infty}{\mu_R} \quad (24)$$

Assuming

$$\frac{\rho_o}{\rho_\infty} = C_6 u_\infty^{0.6} \quad (25)$$

$$\frac{\mu_o}{\mu_R} = \left(\frac{h_o}{h_R} \right)^{0.36} \quad (26)$$

(24) becomes

$$\left(\frac{R_{e\theta}}{F_3}\right)^2 = C_7 \frac{h_R}{u_R}^{0.36} \rho_\infty u_\infty^{0.88} \quad (27)$$

Substituting (3) into (27) gives

$$\left(\frac{R_{e\theta}}{F_3}\right)^2 = C_8 \sin \theta_E \left(\frac{W}{C_D A}\right) \left(\ln \frac{u_E}{u_\infty}\right) \left(\frac{u_\infty}{u_E}\right)^{0.88} u_E^{0.6} u_E^{0.28} \quad (28)$$

Defining

$$N = \left(\ln \frac{u_E}{u_\infty}\right) \left(\frac{u_\infty}{u_E}\right)^{0.88} \quad (29)$$

(28) becomes

$$N = \frac{\left(\frac{R_{e\theta}}{F_3}\right)^2}{\left(\frac{W}{C_D A}\right) C_9 \left(\frac{u_E}{23,477}\right)^{0.28} \left(\frac{\sin \theta_E}{0.35}\right) \frac{(\rho_o/\rho_\infty)_E}{18.2}} \quad (30)$$

or, at transition,

$$N_{TR} = \frac{\left(\frac{R_{e\theta_{TR}}}{F_3}\right)^2}{\left(\frac{W}{C_D A}\right) C_{N_{TR}}} \quad (31)$$

where

$$C_{N_{TR}} = C_9 \left(\frac{u_E}{23,477} \right)^{0.28} \left(\frac{\sin \theta_E}{0.35} \right) \frac{(\rho_o/\rho_\infty)_E}{18.2} \quad (32)$$

The reference enthalpy and viscosity are given by

$$\begin{aligned} h_R &= 2,340,000 \text{ ft-lb/slug} \\ \mu_R &= 0.551 \times 10^{-6} \text{ slug/ft-sec} \end{aligned}$$

Then

$$C_9 = 60,000 \text{ ft/lb}$$

Only one branch of (29) is entered in the program: $(u_\infty/u_E) = 0.32$ to $(u_\infty/u_E) = 1$. At $(u_\infty/u_E) = 0.32$, a peak of $N = 0.41802$ occurs, hence, there is no $u_{\infty_{TR}}$ for body stations at which $N_{TR} > 0.41802$, indicating that only laminar heat transfer is experienced at these stations. To prevent the possibility of aft stations becoming laminar (through the mechanical use of (31) once a more forward station has become turbulent, N_{TR} is compared with the value of N_{TR} at the preceding station (N_{TR}'). If $N_{TR} \geq N_{TR}'$, then the value of N_{TR}' is used to force turbulence at least as soon as it occurs at the immediate forward station. If $N_{TR} < N_{TR}'$, then the program uses N_{TR} .

VII. HEAT SHIELD AND INSULATION THICKNESSES⁽³⁾

The basic Fourier heat conduction equation is used:

$$\frac{\partial^2 T}{\partial x^2} = \frac{1}{\alpha} \frac{\partial T}{\partial t} \quad (33)$$

and it is assumed that the heat shield is a semi-infinite slab. Ablation is accounted for by the designation of a moving surface in the boundary conditions. It can be shown that for a heat input to the surface of the form

$$\dot{q} = \dot{q}_m \left(\frac{t_o}{t} \right)^{1/2} \quad (34)$$

the following equation holds for the normalized velocity of ablation

$$V^* = V_o \left(\frac{t_o}{t} \right)^{1/2} \quad (35)$$

where V_o is determined from

$$\frac{\sqrt{\pi} (1 - V_o) \sqrt{a t_o} \dot{q}_m}{k (T_s - T_o)} \exp \left(\frac{\dot{q}_m^2 t_o V_o^2}{a \rho_M^2 L^2} \right) \operatorname{erfc} \left(\frac{\sqrt{t_o} \dot{q}_m V_o}{\sqrt{a} \rho_M L} \right) = 1 \quad (36)$$

The quantity $\dot{q}_m \sqrt{t_o}$ is found by integrating equation (34) over the total time of heating to yield

$$Q_T = 2 \sqrt{t_f} \left(\dot{q}_m \sqrt{t_o} \right) \quad (37)$$

where Q_T is determined from the procedure of the preceding section and t_f is the total heating time. Once $\left(\dot{q}_m \sqrt{t_o} \right)$ and V_o are known it is then possible to solve for the thickness of material ablated, $\tau_{H.S. ABL.}$:

$$\tau_{H.S. ABL} = 2 \sqrt{a t_f} \frac{\left(\dot{q}_m \sqrt{t_o} \right) V_o}{\rho_M L \sqrt{a}} \quad (38)$$

If the heat shield and insulation have similar thermal properties, the total wall thickness prior to ablation, x_T , can be found from the following equation:

$$\frac{T_i - T_o}{T_s - T_o} = \frac{\operatorname{erfc}\left(\frac{x_T}{2\sqrt{a}t_f}\right)}{\operatorname{erfc}\left(\frac{\tau_{H.S. ABL.}}{2\sqrt{a}t_f}\right)} \quad (39)$$

If the thermal properties of the heat shield and insulation are different and if the insulation cannot exceed some given temperature, $T_{i_{\max}}$, then the total heat shield thickness, $\tau_{H.S. \max}$, can be determined from

$$\frac{T_{i_{\max}} - T_o}{T_s - T_o} = \frac{\operatorname{erfc}\left(\frac{\tau_{H.S. \max}}{2\sqrt{a}t_f}\right)}{\operatorname{erfc}\left(\frac{\tau_{H.S. ABL.}}{2\sqrt{a}t_f}\right)} \quad (40)$$

The total insulation thickness, $\tau_{INS.}$, is then given by

$$\tau_{INS.} = \left(x_T - \tau_{H.S. \max}\right) \left(\frac{a_{INS.}}{a_{H.S.}}\right)^{1/2} \quad (41)$$

where it is assumed that the $\rho_M C_P$ product of the two materials is constant.

VIII. VEHICLE GEOMETRY

The vehicle shape is defined as follows (see Figure 1):

- a) A spherical segment, either solid or hollow.
- b) An arbitrary number of (at least one but not more than ten) conical frustums.
- c) A cover plate at the rear of the vehicle which may be either convex (dashed line) or concave (solid line)

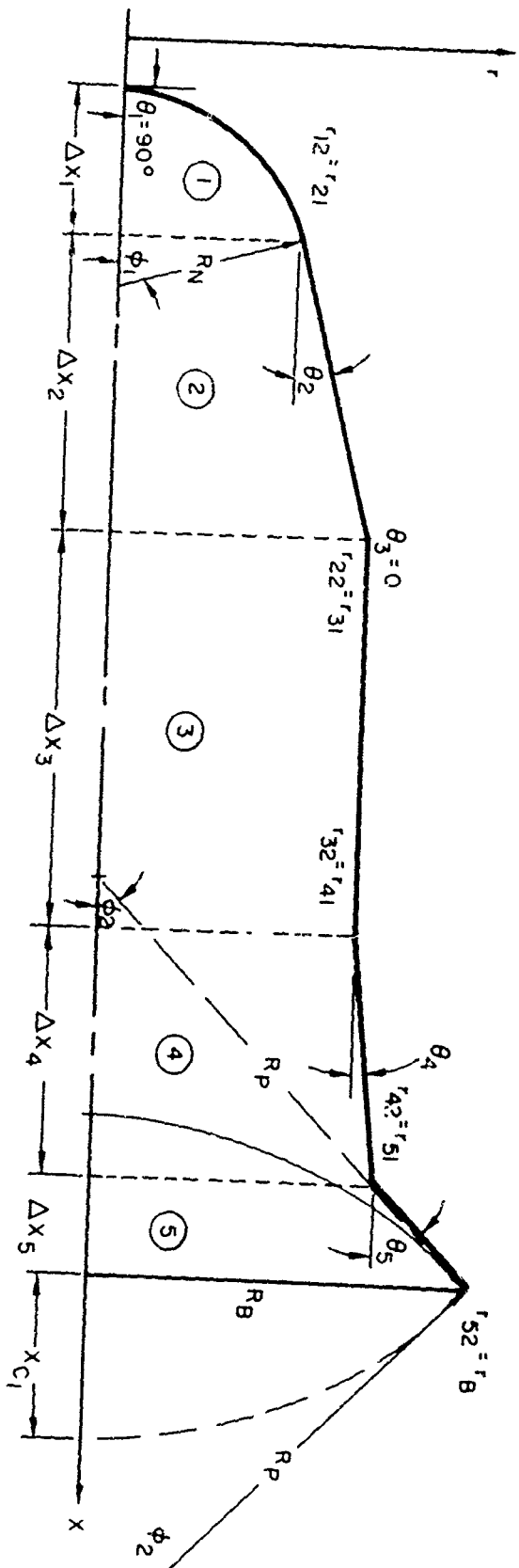


Figure 1. Vehicle Geometry.

The number of computational intervals in each section of (a) and (b) can be arbitrarily chosen from one to eighteen. The number of frustums and the following quantities must be specified to determine the geometry of the vehicle.

- a) R_N must always be specified. If ϕ_1 is not given it will be assumed equal to $(\pi/2 - \theta_2)$, which is the tangent case.
- b) θ_2 is always specified but in any other (i^{th}) section any two of the quantities $(\theta_i, \Delta x_i, R_{i2})$ may be selected. x_{i1} and R_{i1} are computed by the program.
- c) ϕ_2 is assumed specified and $R_P = f(\phi_2, R_B)$. Provision is made for the selection of R_P and the determination of $\phi_2 = f(R_P, R_B)$. When either ϕ_2 or R_P are given as negative the cover plate will be defined as convex.

If the nose cone is specified as solid it will be assumed to be heat sink material, with the radius of the spherical segment equal to $R_N + (\tau_{H.S.} + \tau_{INS.})$ at the juncture of the first section plus τ_{ST} if the structure is on the outside.

All the point radii will be normalized by R_B . It will be assumed that the vehicle geometry does not change for consecutive runs unless specified and then only as specified.

IX. FIXED WEIGHT AND PAYLOAD

An arbitrary amount of fixed weight and payload can be defined in each section. The center of gravity (\bar{x}) of the payload is measured in inches from the front of the frustum in which it is located; the \bar{x} of the fixed weight is taken to be at the \bar{x} of the section, independent of the distribution of the fixed weight. The pitch and roll moments of inertia of the payload are given about the payload center of gravity; the I_P and I_R of the fixed weight are given about the section center of gravity determined without the fixed weight.

Axial symmetry is assumed for the entire vehicle. It will be assumed that these values do not change for consecutive runs unless otherwise specified.

X. MACHINE COMPUTATIONS

This section and Section XI describe the computation procedure of the machine. The various sections of the total computation are listed below. These should be used with the corresponding flow diagrams given in Section XI to understand the procedure of any given section of the computation. The sections below are listed in the order in which they occur during the computation and the chain of computations is shown on the first diagram in Section XI.

A. SHAPE (Body geometry calculation)

This portion of the program determines the geometry of the vehicle from the inputs described in Section VIII. The coordinates of the points (x/R_B , r/R_B) are computed and stored in the point bins. At present the program divides each section into ten intervals. No flow diagram is included since the computation is quite straightforward because of the simple geometries involved. A complete set of applicable flow diagrams is contained in Section X.

B. PRESS (Pressure distribution calculation)

The pressures on the vehicle are supplied to the program by means of linear interpolation from tables of pressures, for Mach 20 and altitudes of 100,000 ft and 65,000 ft. For the first two sections these are pressure values for sphere-cone combinations that have been determined by a method of characteristics solution, and are an integral part of the program. For the remaining sections the pressure tables are a part of the input. If desired, a Newtonian table of pressures which is provided in the program may be used for the remaining sections.

C. FFF (Body function calculations)

The expressions to be computed are F_1 , F_2 , F_3 , as given by equations (9), (19), and (23). The computational procedure is outlined on the included flow diagram.

D. CPM (Cover plate calculations)

The following quantities associated with the cover plate are computed:

$$\bar{x} = x_B - \frac{R_P}{2} (1 - \cos \phi) = \frac{x_{C_1} + x_B}{2}$$

$$W_{ST} = \frac{2\pi}{12^3} \rho_{ST} \tau_{ST} R_P^2 (1 - \cos \phi) = \frac{2\pi}{12^3} \rho_{ST} \tau_{ST} R_P (x_B - x_{C_1})$$

$$I_r = \frac{W}{3g} R_P^2 (2 - \cos \phi - \cos^2 \phi) \cdot \frac{1}{12^2}$$

$$I_x = \frac{W}{3g} \frac{R_P^2}{12^2} (1 + \cos \phi + \cos^2 \phi) + \frac{W}{12^2 g} \left[\bar{x}^2 - (x_1 + R_P - \bar{x})^2 \right]$$

All densities are given in lb/ft³. Lengths are given in inches and weights are given in pounds. The moments of inertia will have the units of slug-ft². The computational procedure is outlined on the included flow diagram.

E. ARDC (Aerodynamic coefficient calculations)

The following Newtonian aerodynamic coefficients associated with the vehicle are computed:

$$C_D = \frac{3.92}{R_B} \int_0^{R_B} \left(\frac{r}{R_B} \right) \left(\frac{P}{P_o} \right) dr$$

$$C_D^{(N)} = \frac{3.92}{R_B} \int_0^{R_B} \left(\frac{r}{R_B} \right) \sin^2 \theta dr$$

$$C_{N_a} = \frac{3.92}{R_B} \int_0^{R_B} \left(\frac{r}{R_B} \right) \cos^2 \theta dr$$

$$C_{M_a} = \frac{3.92 R_B}{x_B R_B} \int_0^{R_B} \left(\frac{r}{R_B} \right) \left[\sin \theta + \left(\frac{x}{R_B} \right) \cos \theta \right] (\cos \theta) dr$$

$$x_{C.P.} = - \frac{C_{M_a}}{C_{N_a}} x_B$$

Since these are straightforward calculations no flow diagram is included

F. ITC (Iterative stagnation pressure calculation)

The equation currently being used for this program is

$$P_o = 3.8 \times 10^{-9} \left(\frac{W}{C_D A} \right) u_E^2 \sin \theta_E$$

where $u_E = 23,477$ ft/sec and $\theta_E = 20.5^\circ$. This value of P_o corresponds to P_o at maximum dynamic pressure.

G. STRG⁽⁴⁾ (Structure calculations)

The structure thickness τ_{ST} , the structural weight W_{ST} , the stiffener ring depth d_{SR} , and stiffener ring weight W_{SR} are computed. This section of the computation considers only the hollow nose; the case of the solid nose is included later.

For the nose:

$$\tau_{ST} = 2.05 R_N \left(\frac{P_o}{E} \right)^{1/2}$$

$$W_{ST} = \frac{2\pi}{12^3} \rho_{ST} \tau_{ST} R_N x_{12}$$

$$d_{SR} = \left(2 \frac{f_{SR}}{\sigma_{SR}} \frac{P_o}{E} R_{12}^3 x_{12} \right)^{1/4}$$

$$W_{SR} = \frac{2\pi}{12^3} \sigma_{SR} \rho_{ST} d_{SR}^2 \left(R_{12} - \frac{d_{SR}}{2} \right)$$

For the frustums:

$$\tau_{ST} = \frac{1}{\cos \theta} \left[\left(\frac{P}{E} \right)^2 (x_{i2} - x_{i1})^2 (R_{i1} + R_{i2})^3 \right]^{1/2}$$

$$W_{ST} = \frac{\pi}{12^3 \cos \theta} \rho_{ST} \tau_{ST} (x_{i2} - x_{i1}) (R_{i1} + R_{i2})$$

$$d_{SR} = \left[2 \frac{f_{SR}}{\sigma_{SR}} \frac{P}{E} R_{i2}^3 (x_{i2} - x_{i1}) \right]^{1/4}$$

$$W_{SR} = \frac{2\pi}{12^3} \sigma_{SR} \rho_{ST} d_{SR}^2 \left(R_{i2} - \frac{d_{SR}}{2} \right)$$

Each stiffener ring joins two consecutive sections, including one joining the nose to the first frustum and one joining the last frustum to the cover plate.

In the above equations, f_{SR} is a safety factor which is assumed to be 1.25 for all computations. The modulus of elasticity E may be varied from section to section. The σ_{SR} is a thickness/depth ratio, τ_{SR}/d_{SR} , for the stiffener rings. The pressure P is taken to be the maximum value of pressure in the section under consideration.

H. THSN (Cold wall heat sink thickness calculation)

In this section the value of $\tau_{C.W} / R_B$ is computed as

$$\frac{\tau_{C.W}}{R_B} = \frac{Q_T}{Q^* \rho_{H.S.} R_B}$$

This implies only cold wall heating with no conduction of heat into the body. The $\tau_{C.W}$ thus found differs from the value of $\tau_{H.S.}$ given in the output. By a later sophistication of the program only the value of Q_T (total heat transferred to the body at any point) is computed. This value is then used as input to equation (37).

In the computation of Q_T the criterion used to determine whether heating is laminar or turbulent is the value of the transition parameter N_{TR} , defined as

$$N_{TR} = \frac{1}{\Delta_i C_{N_{TR}}} \left[\frac{R_{E\theta_{TR}}}{F_3 (r/R_B)} \right]^2$$

$R_{E\theta_{TR}}$ is given as input for each case and $C_{N_{TR}}$ is defined as.

$$C_{N_{TR}} = 6.00 \times 10^4 \left[\left(\frac{u_E}{23,477} \right)^{0.28} \left(\frac{\sin \theta_E}{0.35} \right) \frac{\left(\frac{\rho_o}{\rho_\infty} \right)_E}{18.2} \right]$$

where $\left(\rho_o / \rho_\infty \right)_E$ is a tabulated linear function of u_E . The equation for Q_T (see flow diagram and N.T.C. calculation sheet) is

$$Q_T = Q^* \rho_{H.S.} (H.S.B.) d \left\{ (HSC) F_1 \operatorname{erf}(\xi) + e \left[\Gamma_{X_{CO}} \left(\frac{4}{5} \right) - \Gamma_{X_{TR}} \left(\frac{4}{5} \right) \right] F_2 \right\}$$

where

$$\xi = \left(2.152 \ln \frac{u_E}{u_\infty} \right)^{1/2}$$

This equation is modified for the various values of N_{TR} as follows:

for $N_{TR} \geq 0.4179$, set $\operatorname{erf}(\xi) = 1$ and $\Gamma_{X_{TR}} \left(\frac{4}{5} \right) = \Gamma_{X_{CO}} \left(\frac{4}{5} \right)$

$N_{TR} \geq N_{TR}'$ then use N_{TR}'

$N_{TR} < N_{TR}'$ then use N_{TR}

There are tables stored in the computer giving:

$$\left(\frac{u_\infty}{u_E} \right) = f(N_{TR})$$

$$\operatorname{erf}(\xi) = f \left(\frac{u_\infty}{u_E} \right)$$

$$\Gamma_{X_{TR}} \left(\frac{4}{5} \right) = f \left(\frac{u_\infty}{u_E} \right)$$

I. TINSR (Heat sink and insulation thickness calculation)

For this computation equation (37) is interpreted as:

$$Q_T = 2\sqrt{t_f} (\dot{q}_m \sqrt{t_o}) = (\tau_C w.) (\rho_{H.S.}) (Q^*)$$

from which $\dot{q}_m \sqrt{t_o}$ is found. The value of t_f in this computation is currently given in the program as 30 seconds. This value of $\dot{q}_m \sqrt{t_o}$ is substituted into equation (36) giving

$$\frac{\sqrt{a_{H.S.}} \pi Q^* \tau_{cw} \rho_{H.S.} (1 - V_o)}{2\sqrt{t_f} k (T_s - T_o)} \exp \left(\frac{Q^* \tau_{cw}}{2\sqrt{t_f} a_{H.S.} L} \right)^2 V_o^2 \operatorname{erfc} \left(\frac{Q^* \tau_{cw}}{2\sqrt{t_f} a_{H.S.} L} \right) V_o = 1$$

or, in terms of the constants defined on the flow diagram,

$$K_3 (1 - V_o) \exp (K_2 V_o^2) \operatorname{erfc} K_1 V_o = 1$$

With the introduction of the new variable $V_o^* = V_o K_1$, this equation becomes:

$$g(V_o^*) = \frac{K_3}{K_1} (K_1 - V_o^*) \exp V_o^{*2} \operatorname{erfc} V_o^* - 1 = 0$$

which is the equation utilized by the computer. If $V_o^* > 3$ the quantity $\operatorname{erfc} V_o^*$ must be computed by the complementary error function routine on the computer for accuracy. If $V_o^* < 3$ the faster computer route for $\operatorname{erf} V_o^*$ may be used and the result subtracted from 1.

The value of V_o^* for which $g(V_o^*) = 0$ must now be found. It is easily seen that $g(0) = K_3 - 1$ and $g(K_1) = -1$, so that the required value of V_o^* lies between 0 and K_1 if $K_3 > 1$. A binary search is conducted for the root of $g(V_o^*)$; the V_o^* selected is that for which the absolute value of the difference between consecutive values of V_o^* is less than 0.01.

The thickness of heat sink ablated is then computed from equation (38). Then equation (39) can be solved. If $\eta > 8.5$ the value of $\tau_{INS.}$ is extremely small—as indicated by equations (39), (40), and (41)—and $\tau_{INS.}$ is set equal to the minimum specified value of 0.1 inch. The

computational method to determine $\text{erfc } \eta$ is analogous to that described above for $\text{erfc } V_o^*$. If the ablation temperature is equal to or less than the maximum permissible inside wall temperature, the computed value of $\tau_{\text{INS.}}$ would be zero; thus $\tau_{\text{INS.}}$ is again set equal to the minimum specified value of 0.1 inch.

In the section of the flow diagram enclosed in the dashed lines a binary search is conducted for x_T , which is the total wall thickness for homogeneous material construction, provided the computed $\tau_{\text{INS.}} > 0.1$ inch. This quantity is found just before the flag check is entered for the first time.

The program then proceeds out of the flag check on the path marked (1) and checks to determine whether $T_{i\text{max}} = T_s$. If so, the insulation and heat sink are of the same material and $\tau_{\text{INS.}}$ is computed as shown. If not, the heat sink and insulation materials are different. After the flag is changed to show that x_T routine is completed and the changes noted on the flow diagram are made, the procedure enclosed in the dotted lines is again utilized to compute the total heat sink thickness, $\tau_{\text{H.S. max}}$. The $\tau_{\text{INS.}}$ is then computed as shown for the case of different insulation and heat sink materials.

J. NSH (Heat sink and insulation weight calculations)

In this section of the computations the weights of the heat sink and insulation materials for a hollow nose, solid nose, and the frustums are determined.

For the solid nose:

$$W_{\text{H.S.}} = \frac{2\pi \rho_{\text{H.S.}}}{12^3 \cdot 3} (R_N + \tau^*) (1 - \cos \phi_1)$$

$$W_{\text{INS.}} = 0$$

where $\tau^* = \tau_{INS} + \tau_{H.S.}$ at the juncture with the first section plus τ_{ST} if the structure is on the outside of that section

In the case of the hollow sections the following computational technique is used:

$$\tau_{INS.} = \tau_K \text{ to compute } \frac{W_1}{\rho_M}$$

$$\tau_{INS.} + \tau_{H.S.} = \tau_K \text{ to compute } \frac{W_2}{\rho_M}$$

Then the heat sink and insulation weights are determined from the following relationships.

$$W_{INS} = \frac{W_1}{\rho_M} \cdot \rho_{INS.} \cdot \frac{1}{12^3}$$

$$W_{H.S.} = \left(\frac{W_2}{\rho_M} - \frac{W_1}{\rho_M} \right) \rho_{H.S.} \cdot \frac{1}{12^3}$$

For the hollow nose:

$$\frac{W}{\rho_M} = 2\pi \int_0^{\phi_1} \left[(R_N + \tau_K \cdot R_B)^3 - R_N^3 \right] \frac{\sin \phi d\phi}{3}$$

where $d\phi = \phi_1/n$ in radians, and R_N is replaced by $(R_N + \tau_{ST})$ if the structure is on the outside of the nose.

For the frustums:

$$\frac{W}{\rho_M} = \pi R_B^2 \int_{x_1}^{x_2} \left[\left(r + \frac{\tau_K}{\cos \theta} \right)^2 - r^2 \right] dx = 2\pi R_B^2 \int_{x_1}^{x_2} \left[r + \frac{\tau_K}{2 \cos \theta} \right] \tau_K ds$$

where

$$ds = \frac{x_2 - x_1}{n(\cos \theta)}$$

K. WTOTS and WTOTB (Iterative ballistic coefficient calculation)

These two operations are straightforward and require no flow diagram. The computation equations are:

$$W_{TOT} = \sum_j [(W_{H.S.})_j + (W_{INS.})_j + (W_{ST})_j + (W_{SR})_j + (W_{P/L})_j + (W_{FIXED})_j]$$

where j denotes a section of the vehicle;

$$A_{TOT} = \frac{\pi}{12^2} \left(R_B + \frac{\tau_{H.S.}}{\cos \theta} + \frac{\tau_{INS.}}{\cos \theta} \right)^2$$

This expression will also include a τ_{ST} term if the structure is on the outside.

The ballistic coefficient is then computed as

$$\Delta_{i+1} = \frac{W_{TOT}}{C_D \cdot A_{TOT}}$$

L. TEST

This section of the computations is explained on the flow diagram

M. XIXIR and IRXIX (Moment calculations)

The equations used for the computations in these sections are given on the flow diagram. The primed quantities refer to volumes rather than masses; that is, I' refers to the volume moment of inertia and M' to the volume first moment. The XIXIR computations are only for the nose and are followed directly by the IRXIX computations for the frustums.

N. MSTR

This set of computations is adequately described by the flow diagram

O. TBM (Tabulation computations)

These computations are straightforward and a flow diagram was not considered necessary.

$$x_{TOT} = \frac{\sum_j W_j (\bar{x})_j}{W_{TOT}}$$

$$I_{P_{TOT}} = \sum_j \left\{ \left(I_x + \frac{I_r}{2} \right)_j + \frac{W_j}{12^2 g} \left[(\bar{x}_{TOT} - \bar{x}_j)^2 - \bar{x}_j^2 \right] + \left(I_{P_{FIXED}} + I_{P_{P/L}} \right)_j \right. \\ \left. + \frac{W_{P/L}}{12^2 g} (\bar{x}_{TOT} - \bar{x}_{P/L})^2 + \frac{W_{FIXED}}{12^2 g} (\bar{x}_{TOT} - \bar{x}_j)^2 \right\}$$

$$I_{R_{TOT}} = \sum_j (I_R)_j$$

These quantities are computed both with and without heat sink weight.

P. ETC (Miscellaneous calculations)

The following Newtonian stability parameters are also computed by the program at the end of the other computations:

$$C_{M_q} = - \frac{3.92 \cdot R_B}{x_B^2} \int_0^{R_B} (r/R_B) \cos 2\theta \left\{ (r/R_B) \tan \theta + \left[\left(\frac{x}{R_B} \right) - \left(\frac{x_{TOT}}{R_B} \right) \right]^2 \right\} dr$$

$$\text{Stab. Par} = \frac{1}{C_D} \left[C_{N_\alpha} - C_D - \left(C_{m_q} + C_{m_\alpha} \right) \frac{\left(\frac{W_{TOT}}{g} \right) \left(\frac{x_B}{12} \right)^2}{I_{P_{TOT}}} \right]$$

$$l = x_B \pm x_{C_1}$$

XI. FLOW DIAGRAMS

This section contains the following flow diagrams:

1. General Control for Computations
 2. FFF Calculations
 - 2a. FFF Calculation Notes
 3. CPM' Calculations
 4. N.T.C. Calculations
 5. STRG Calculations
 6. THSN Calculations
 7. TINSR Calculations
 8. Test
 9. XIXIR Calculations
 10. IRXIX Calculations
 11. MSTR Calculations
-

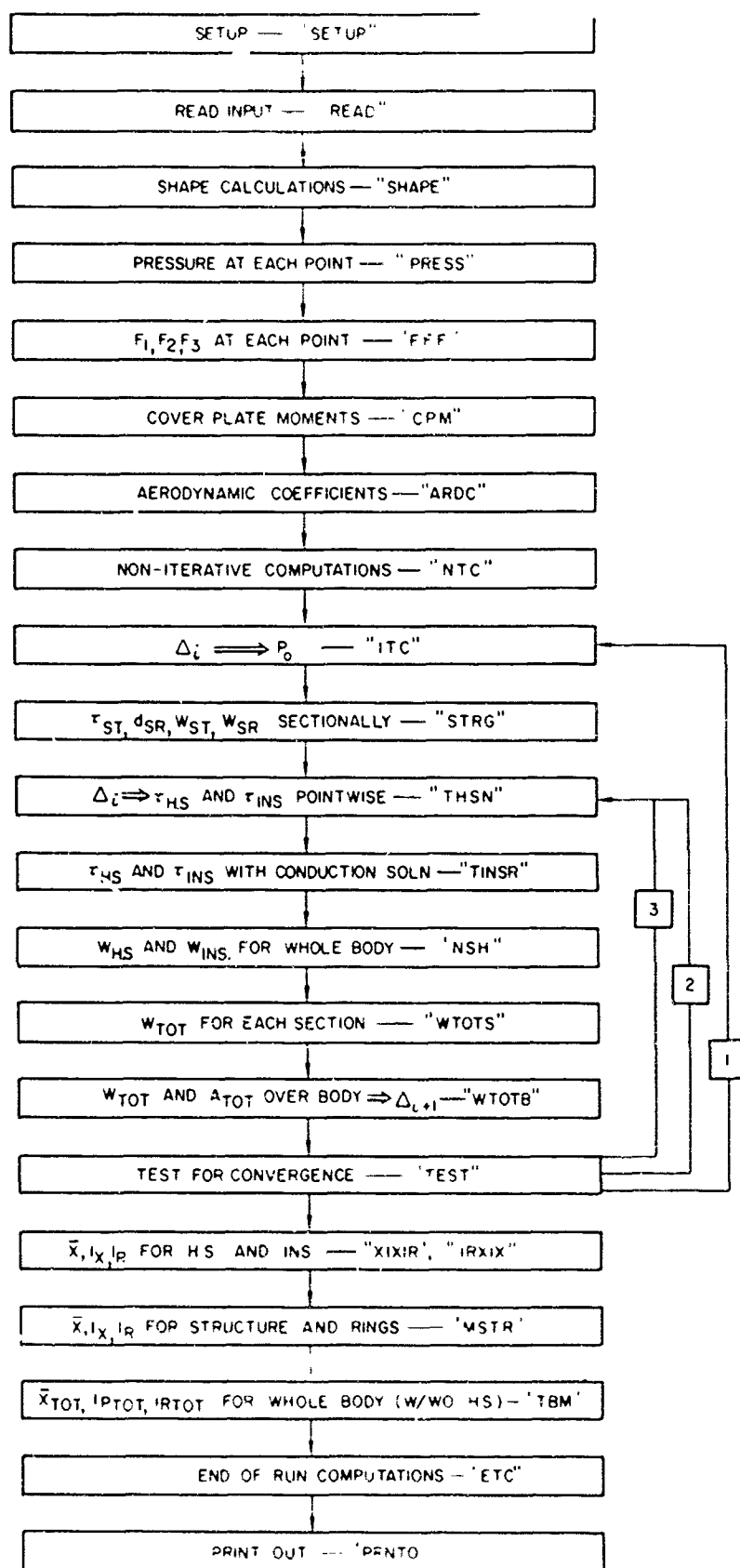


Diagram 1. General Control for Computations.

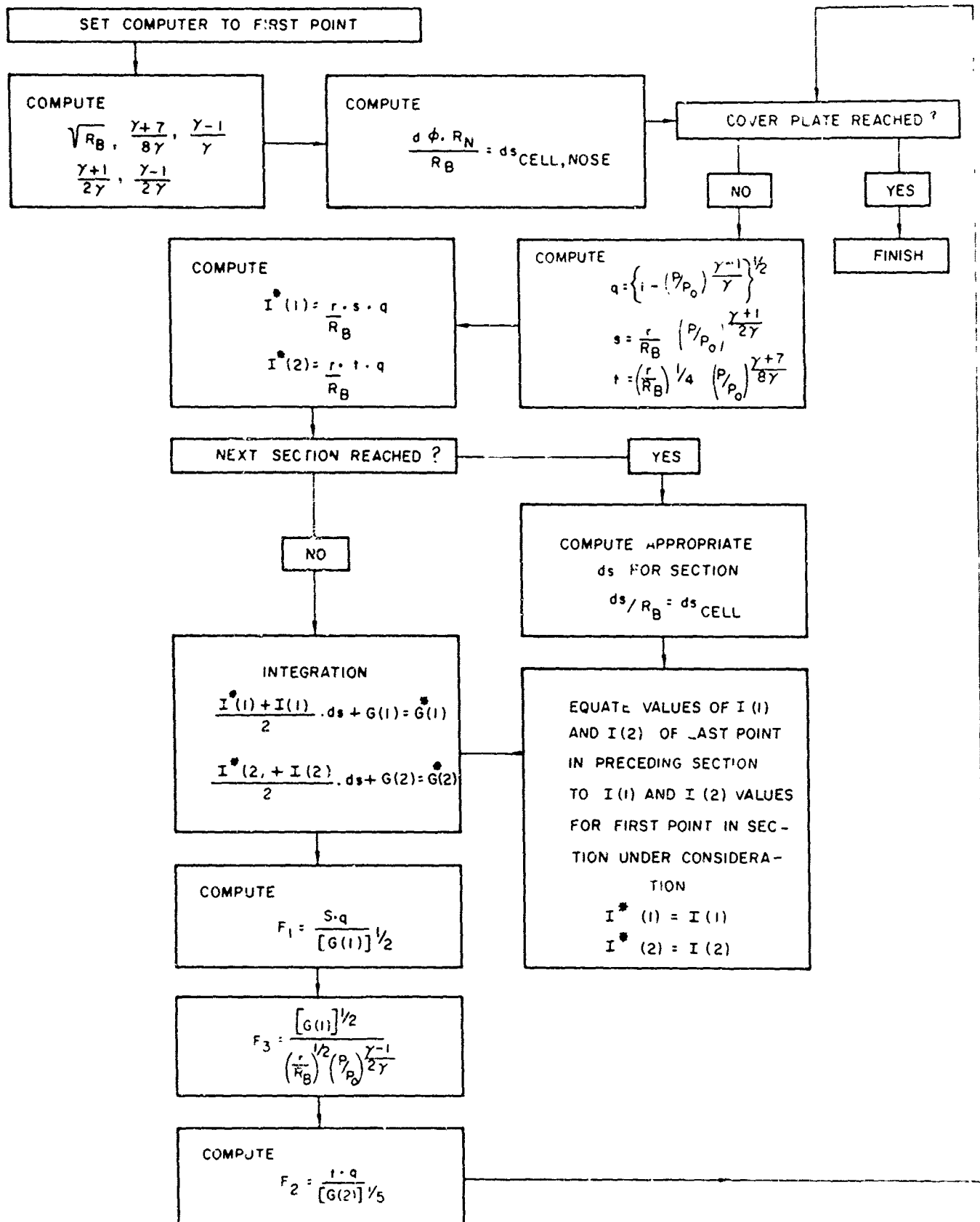


Diagram 2. FFF Calculations.

STARRED QUANTITIES REPRESENT VALUES AT THE POINT
UNDER CONSIDERATION — UNSTARRED QUANTITIES ARE FROM
PRECEDING POINT.

$$G(1) = \int_0^{r/R_B} \left(\frac{r}{R_B} \right)^2 \left(\frac{P}{P_0} \right)^{\frac{\gamma+1}{2\gamma}} \left[1 - \left(\frac{P}{P_0} \right)^{\frac{\gamma-1}{\gamma}} \right]^{1/2} ds$$

$$G(2) = \int_0^{r/R_B} \left(\frac{r}{R_B} \right)^{5/4} \left(\frac{P}{P_0} \right)^{\frac{\gamma+7}{8\gamma}} \left[1 - \left(\frac{P}{P_0} \right)^{\frac{\gamma-1}{\gamma}} \right]^{1/2} ds$$

$$ds_{\text{FRUSTUMS}} = \frac{d \left(\frac{r}{R_B} \right)}{\sin \theta}$$

Diagram 2a. FFF Calculation Notes.

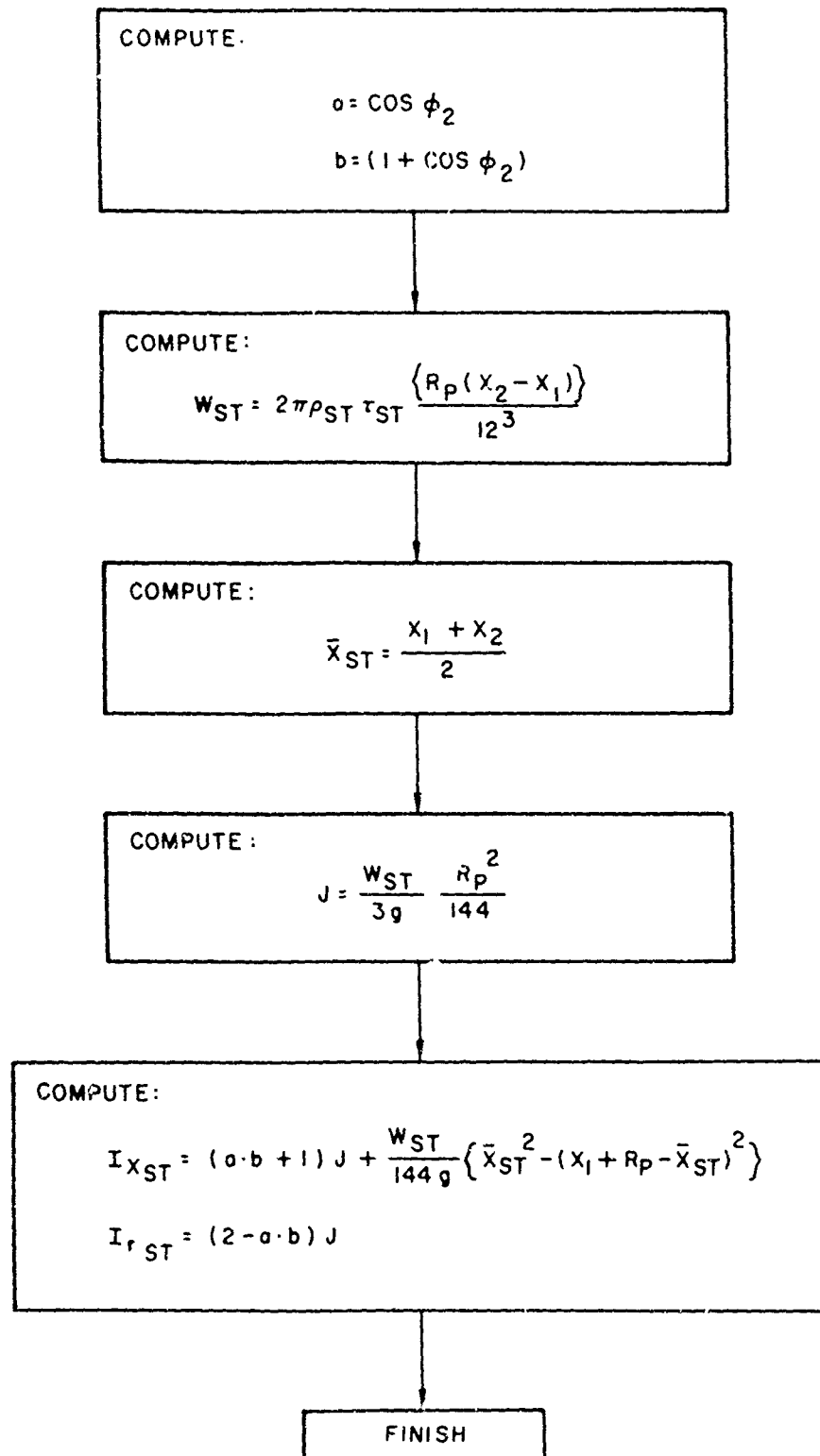


Diagram 3. CPM Calculations.

$$(1) \quad C_{NTR} = 6.00 \times 10^4 \left(\frac{u_E}{23477} \right)^{0.28} \frac{\sin \theta_E}{0.35} \cdot \frac{\frac{P_0}{P_\infty E}}{18.2}$$

WHERE (P_0/P_∞) IS TABULATED VS. u_E IF $h_E \leq 250,000$
— OTHERWISE GO TO ERROR AND STOP.

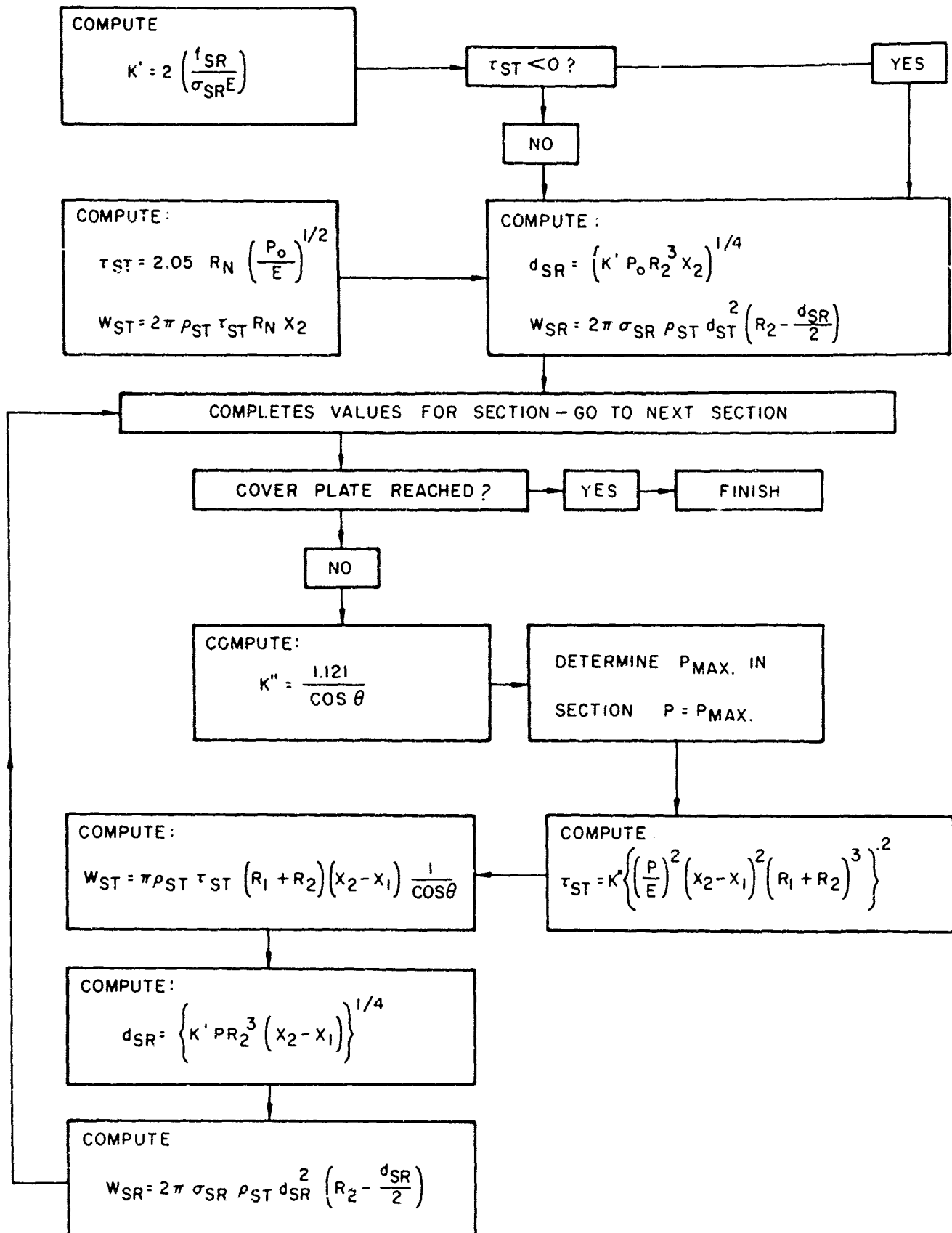
$$(2) \quad HSA = 0.748 \left(\frac{u_E}{23477} \right)^{0.335} \left(\frac{\sin \phi}{0.35} \cdot \frac{R_B}{12} \right)^{0.3}$$

$$(3) \quad HSB = (R_N/R_B)^{1/2}$$

$$(4) \quad HSC = \frac{\left(\frac{\gamma}{\gamma-1} \right)^{1/4}}{2}$$

$$(5) \quad CQL = 899 \left(\frac{u_E}{23477} \right)^{2.15} \left(\frac{0.35}{\sin \phi} \right)^{1/2} = 899 \left(\frac{u_E}{23477} \right)^{2.15} \left(\frac{\sin \phi}{0.35} \right)^{-1/2}$$

Diagram 4. N. T. C. Calculations.



NOTE

① ALL VALUES OF ρ_{ST} USED ARE EQUAL TO $\frac{\rho_{ST}}{12^3}$

Diagram 5. STRG Calculations.

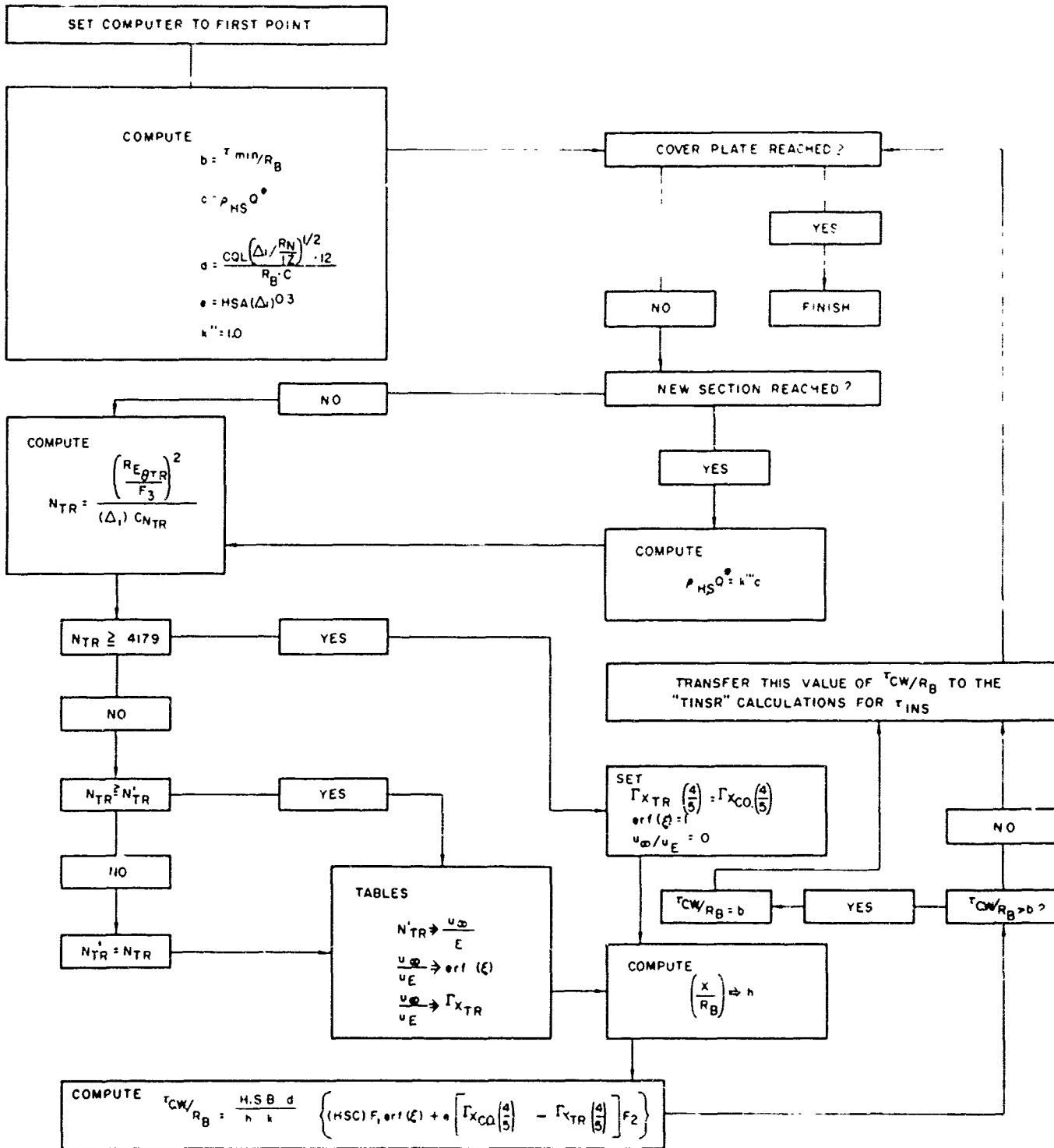
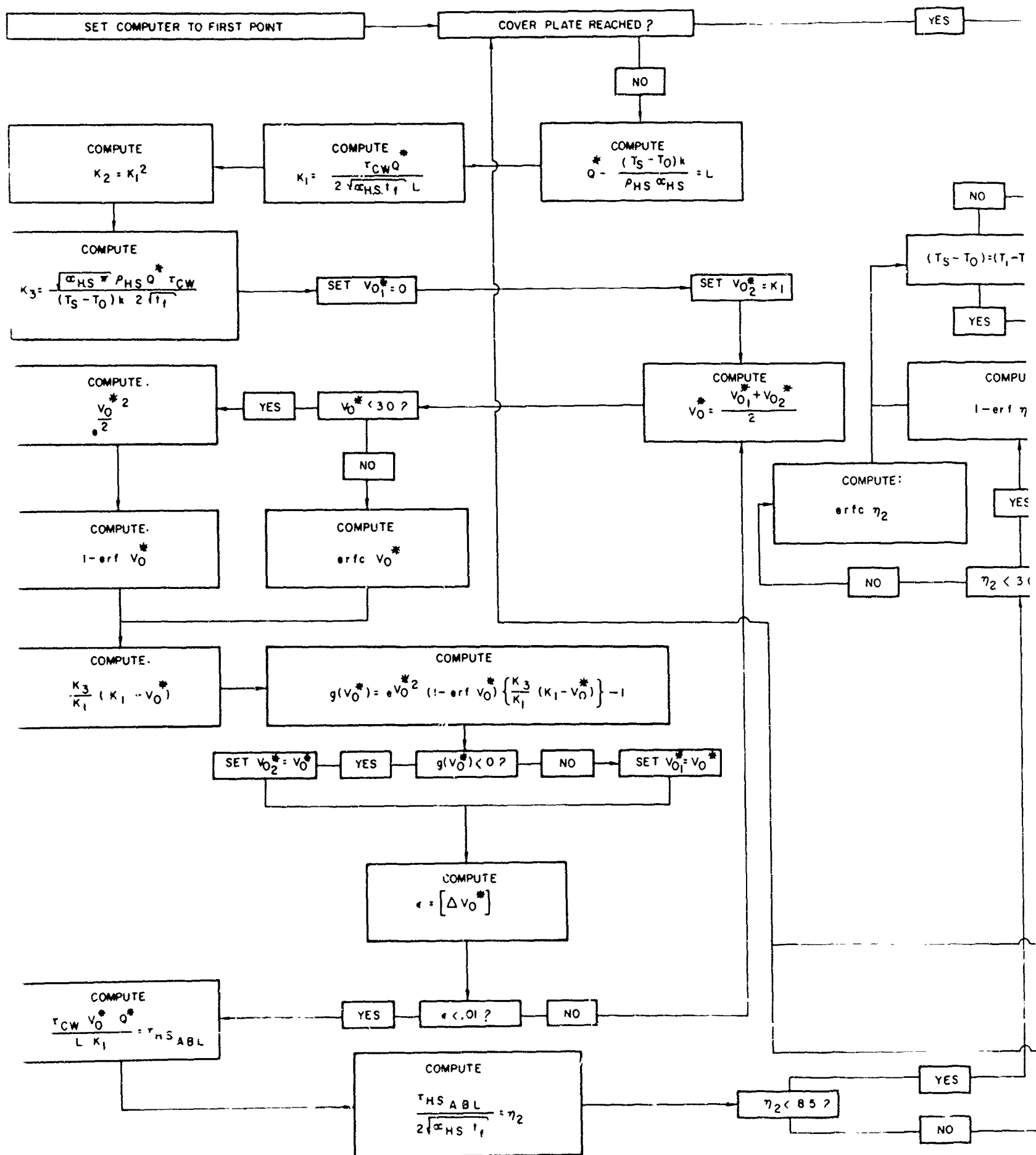


Diagram 6. THSN Calculations.

2
RAMES



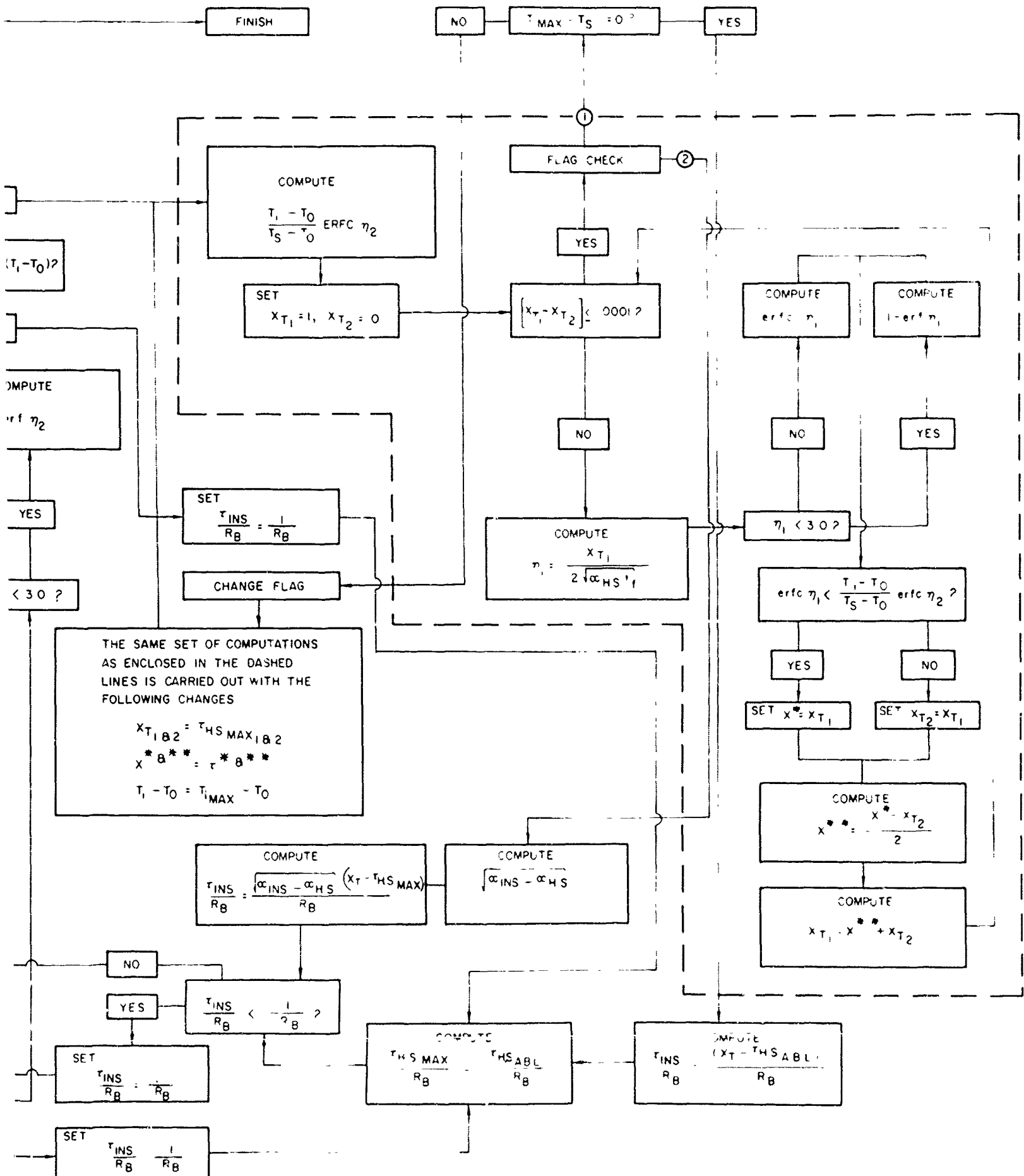
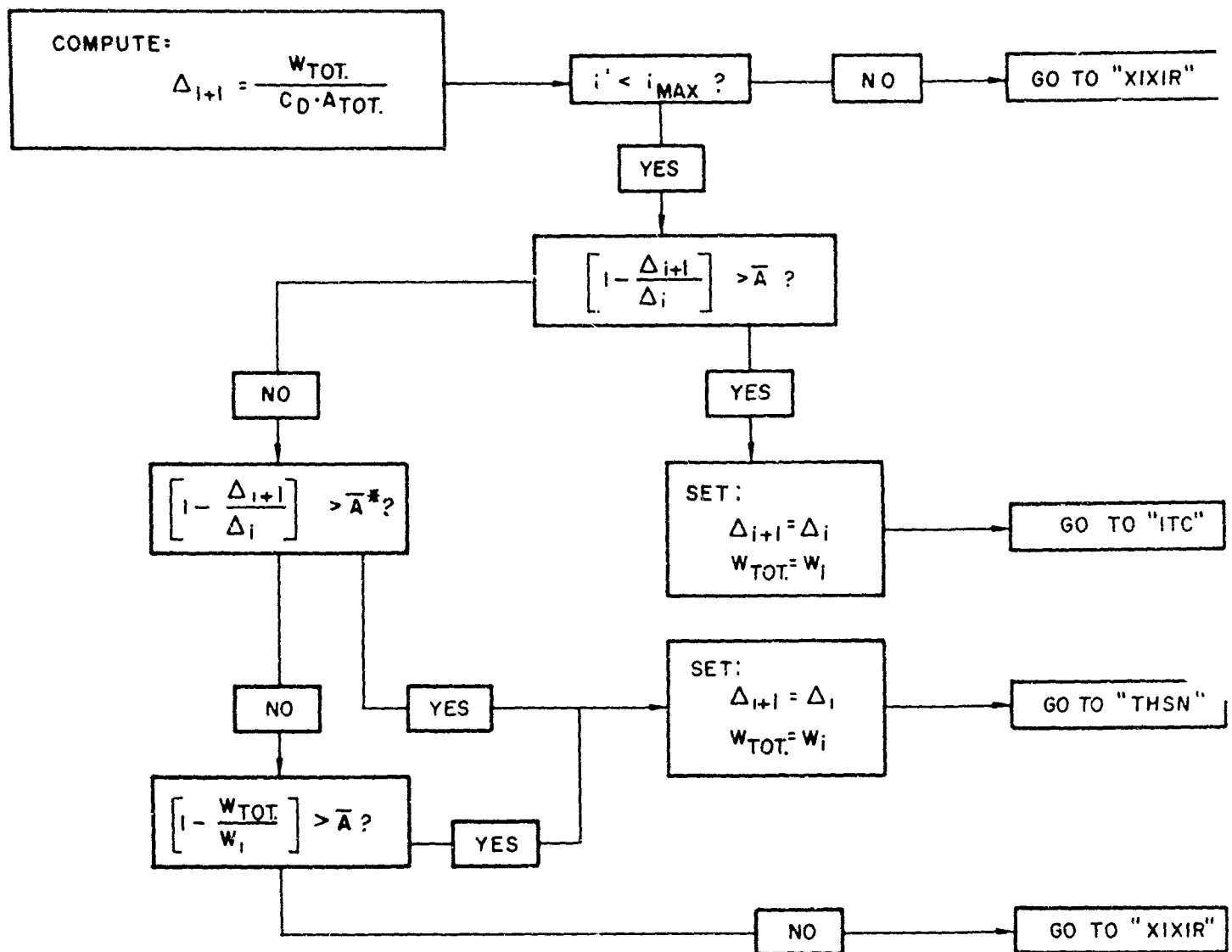


Diagram 7. TINSR Calculations.



NOTE:

$i' = i+1$ IN PRECEDING EQUATION

$\bar{A} = 0.05$ IN CURRENT PROGRAM

$\bar{A}^* = 0.01$ IN CURRENT PROGRAM

THE EQUATION BEING USED FOR "ITC" IN THE CURRENT PROGRAM

IS: $P_0 = 3.8 \times 10^{-9} \Delta u_E^2 \sin \theta_E$

— THE MACHINE THEN PROCEEDS

TO THE "STRG" CALCULATIONS

Diagram 8. Test.

FRAMES

SET COMPUTER TO NOSE

$\tau_{ST} < 0?$

COMPUTE

$$\frac{\rho_{HS} \{M'_{TOT HS + INS} - M'_{HS RES + INS}\} 2\pi}{12^3 W_{HS ABL}} = \bar{X}_{HS ABL}$$

COMPUTE

$$\frac{\rho_{INS} M'_{INS} + \rho_{HS} \{M'_{RES} - M'_{INS}\} 2\pi}{12^3 W_{INS + HS RES}} = \bar{X}_{INS + HS RES}$$

COMPUTE

$$\frac{2\pi}{12^5 g} \rho_{HS} \{I'_{X INS + HS TOT} - I'_{X INS + HS RES}\} = I_{X HS ABL}$$

$$\frac{2\pi}{12^5 g} \left[\{I'_{X INS + HS RES} - I'_{X INS}\} \rho_{HS} + I'_{X INS} \rho_{INS} \right] = I_{X INS + HS RES}$$

COMPUTE

$$\bar{X}_{INS + HS RES} = -$$

$$\bar{X}_{HS ABL} = \frac{2\pi \rho_{HS}}{12^3}$$

COMPUTE

$$\frac{2\pi}{12^5 g} \rho_{HS} \{I'_{R INS + HS TOT} - I'_{R INS + HS RES}\} = I_{R HS ABL}$$

$$\frac{2\pi}{12^5 g} \left\{ \rho_{HS} [I'_{R INS + RES} - I'_{R INS}] + I'_{R INS} \rho_{INS} \right\} = I_{R INS + RES}$$

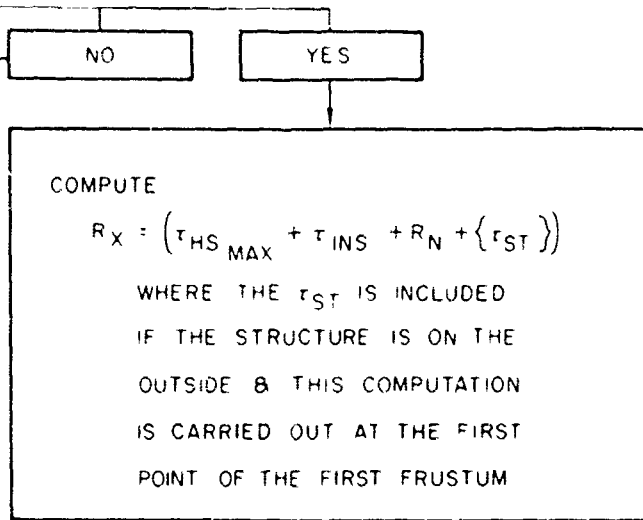
COMPUTE

$$I_{X HS ABL} = \frac{2\pi \rho_{HS}}{12^5 g} \left\{ R_X^3 \left[\frac{R_N^2}{8} \right] \right.$$

$$I_{X INS + RES} = \frac{2\pi \rho_{HS}}{12^5 g} (R_X - \tau_{HS})$$

$$I_{R HS ABL} = \frac{2\pi \rho_{HS}}{12^5 15 g} \left[\frac{\cos^3 \phi}{3} + \right.$$

$$I_{R INS + RES} = \frac{2\pi \rho_{HS}}{12^5 15 g} \left[\frac{\cos^3 \phi}{3} \right.$$



$$= \frac{2\pi\rho_{HS} (R_X - \tau_{HS \text{ ABL}})^3 (\cos \phi - 1)}{12^3 W_{INS} + HS_{RES}} \left\{ \frac{(1 + \cos \phi)}{8} [R_X - \tau_{HS \text{ ABL}}] - \frac{R_N}{3} \right\}$$

$$- \frac{\rho_{HS} (\cos \phi - 1)}{12^3 W_{HS \text{ ABL}}} \left\{ R_X^3 \left[\frac{(1 + \cos \phi)}{8} R_X - \frac{R_N}{3} \right] - (R_X - \tau_{HS \text{ ABL}})^3 \left[\frac{(1 + \cos \phi)}{8} (R_X - \tau_{HS \text{ ABL}}) - \frac{R_N}{3} \right] \right\}$$

$$\frac{R_N^2}{8} + R_X \cos \phi \left(R_X \frac{\cos \phi}{5} - \frac{R_N}{2} \right) - (R_X - \tau_{HS \text{ ABL}})^3 \left[\frac{R_N^2}{8} + (R_X - \tau_{HS \text{ ABL}}) \cos \phi \left(\frac{[R_X - \tau_{HS \text{ ABL}}]}{5} \cos \phi - \frac{R_N}{2} \right) \right]$$

$$\tau_{HS \text{ ABL}}^3 \left\{ \frac{R_N^2}{8} + (R_X - \tau_{HS \text{ ABL}}) \cos \phi \left(\frac{[R_X - \tau_{HS \text{ ABL}}]}{5} \cos \phi - \frac{R_N}{2} \right) \right\}$$

$$\left[\frac{5\phi}{3} + 2 \right] \left\{ R_X^5 - (R_X - \tau_{HS \text{ ABL}})^5 \right\}$$

$$\left[\frac{5\phi}{3} + 2 \right] \left\{ R_X - \tau_{HS \text{ ABL}} \right\}^5$$

COMPLETES NOSE - GO TO FIRST FRUSTUM (RXIX)

Diagram 9. XIXIR Calculations.

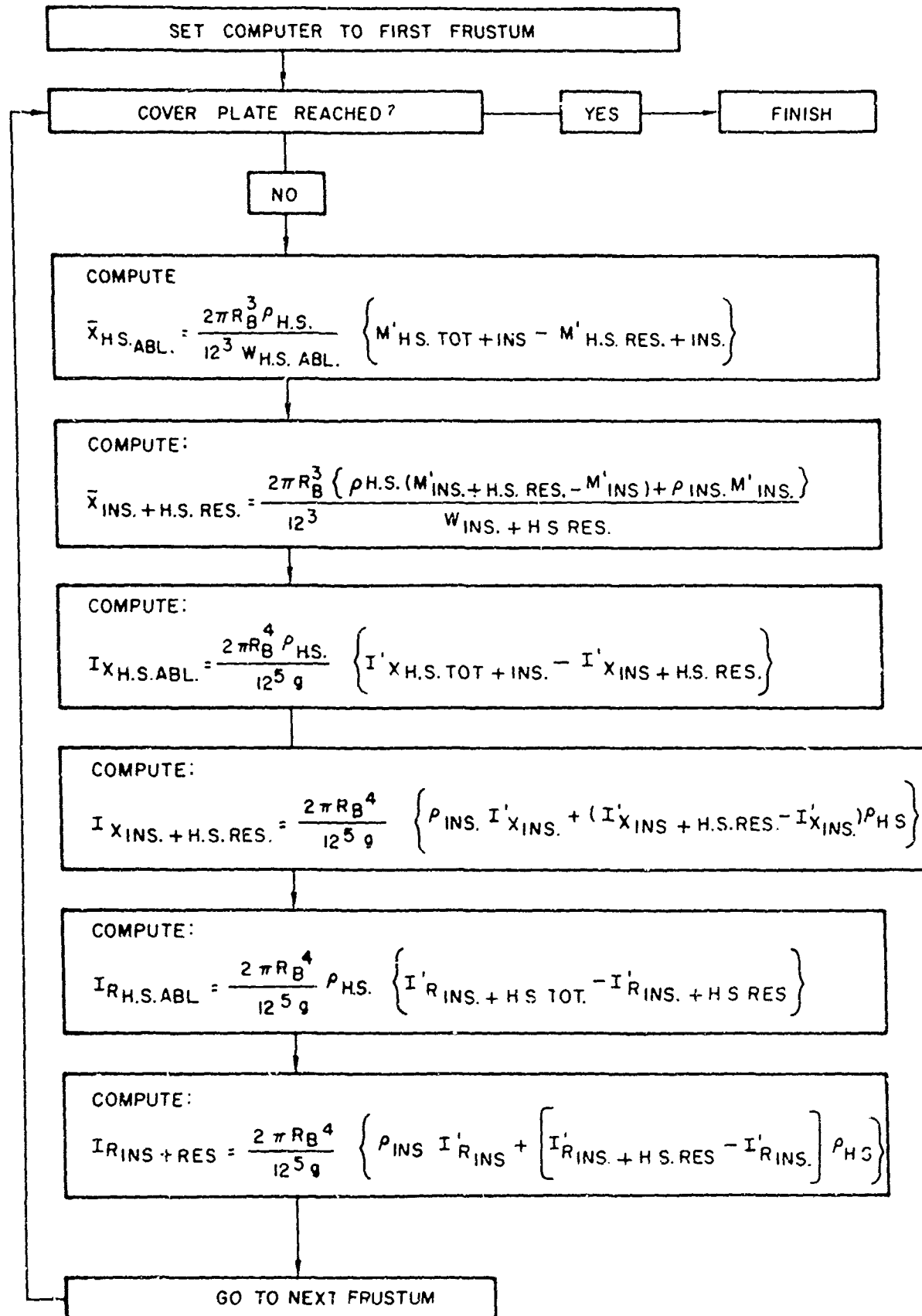
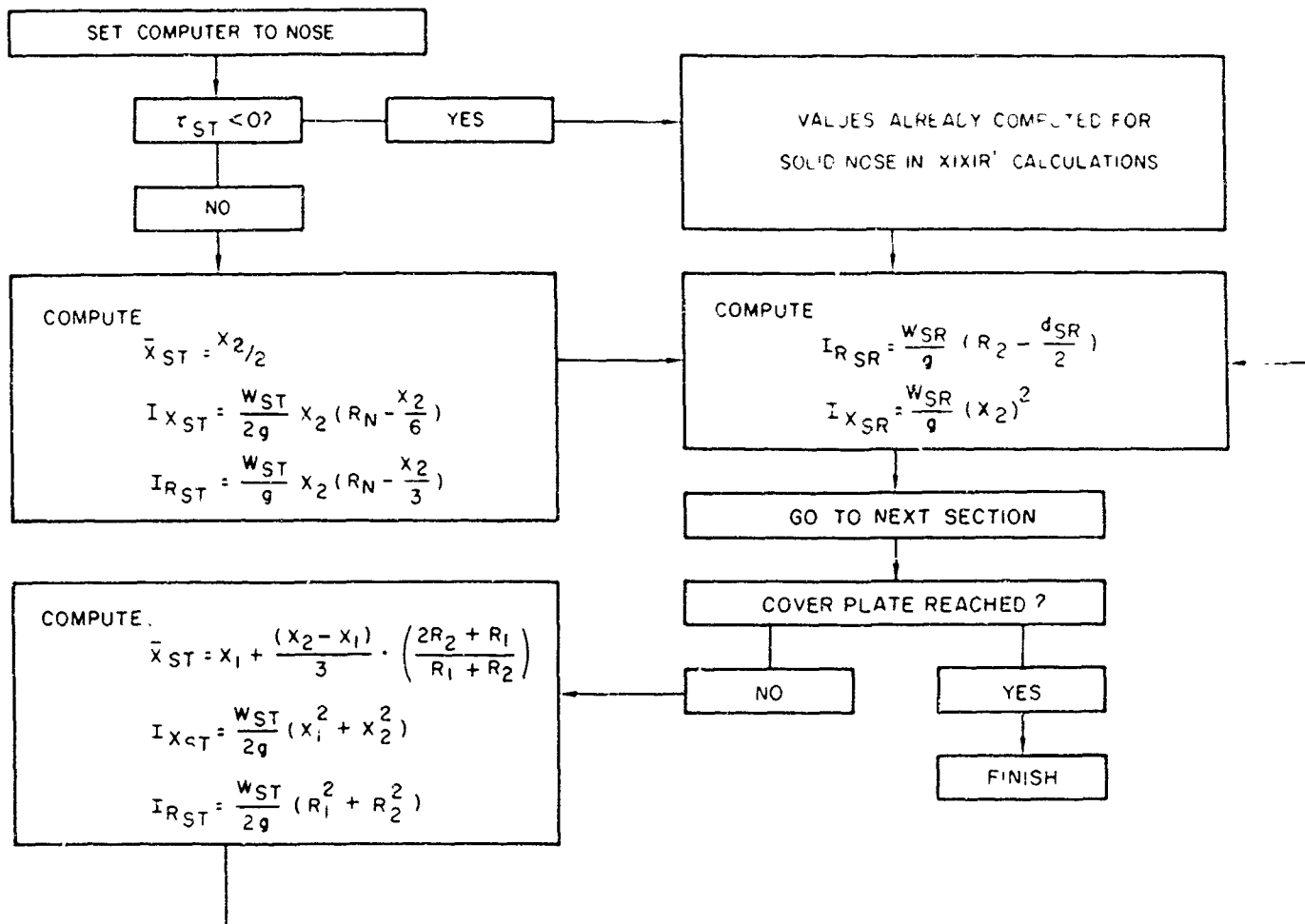


Diagram 10. IRXIX Calculations.



NOTE:

- ① THROUGHOUT CALCULATION USE (144 g) FOR g
- ② ALTHOUGH THE MOMENT VALUES FOR THE RINGS IN THE SOLID NOSE ARE COMPUTED, THEY ARE NOT USED

Diagram 11. MSTR Calculations.

REFERENCES

1. Bromberg, R., J.L. Fox, W.O. Ackerman, "A Method of Predicting Convective Heat Input to the Entry Body of a Ballistic Missile," Ramo-Wooldridge Corporation Report, June 1956.
2. Allen, H.J. and A.J. Eggers, "A Study of the Motion and Aerodynamic Heating of Missiles Entering the Earth's Atmosphere at High Supersonic Speeds," NACA TN4047, August 1953.
3. Baer, D., and A. Ambrosio, "Heat Conduction in a Semi-Infinite Slab with Sublimation at the Surface," Space Technology Laboratories, Inc. Report No. TR-59-0000-00610, February 1959.
4. Zuckerman, I., "Method for Estimating Weights of Sphere-Cone Combinations for Use as Nose Cone Internal Structures," Ramo-Wooldridge Corporation Report No. GM61.1-62, June 1957.

DISTRIBUTION

A. Ambrosio

D.H. Baer

R.P. Berry

C.B. Cohen

J. Doner

G. Harju

A. Jensen

H. Klein

J.B. Peterson

T.L. Petersen (12)

E. Robinson

J.R. Sellars

T.R. Thompson

H.R. Wilkinson